LETTER

https://doi.org/10.1038/s41586-019-1090-x

Astrophysical detection of the helium hydride ion HeH^+

Rolf Güsten[1]*, Helmut Wiesemeyer[1], David Neufeld[2], Karl M. Menten[1], Urs U. Graf[3], Karl Jacobs[3], Bernd Klein[1,4], Oliver Ricken[1], Christophe Risacher[1,5] & Jürgen Stutzki[3]

During the dawn of chemistry[1,2], when the temperature of the young Universe had fallen below some 4,000 kelvin, the ions of the light elements produced in Big Bang nucleosynthesis recombined in reverse order of their ionization potential. With their higher ionization potentials, the helium ions He^{2+} and He^+ were the first to combine with free electrons, forming the first neutral atoms; the recombination of hydrogen followed. In this metal-free and low-density environment, neutral helium atoms formed the Universe's first molecular bond in the helium hydride ion HeH^+ through radiative association with protons. As recombination progressed, the destruction of HeH^+ created a path to the formation of molecular hydrogen. Despite its unquestioned importance in the evolution of the early Universe, the HeH^+ ion has so far eluded unequivocal detection in interstellar space. In the laboratory the ion was discovered[3] as long ago as 1925, but only in the late 1970s was the possibility that HeH^+ might exist in local astrophysical plasmas discussed[4–7]. In particular, the conditions in planetary nebulae were shown to be suitable for producing potentially detectable column densities of HeH^+. Here we report observations, based on advances in terahertz spectroscopy[8,9] and a high-altitude observatory[10], of the rotational ground-state transition of HeH^+ at a wavelength of 149.1 micrometres in the planetary nebula NGC 7027. This confirmation of the existence of HeH^+ in nearby interstellar space constrains our understanding of the chemical networks that control the formation of this molecular ion, in particular the rates of radiative association and dissociative recombination.

The planetary nebula NGC 7027 seems a natural candidate for a search for HeH^+: the nebula is very young (with a kinematic age of only 600 years)[11], and its shell of released stellar material is still rather compact and dense. The central star is one of the hottest known (with an effective temperature, $T_{\rm eff}$, of some 190,000 K) and is very luminous (with a luminosity of $1.0 \times 10^4\ L_\odot$, where $L_\odot$ is the luminosity of the Sun)[12]. Under these conditions, the Strömgren spheres that are created by the hard intense radiation field of the nebula's central hot white dwarf are not yet fully developed, and the radiation field drives ionization fronts into the molecular envelope. The He^+ Strömgren sphere will extend slightly beyond the H^+ zone, and it is in this thin overlap layer that HeH^+ will be produced. Detailed calculations[13] led to predictions for the intensities of the $v = 1$–0 R(0) and P(2) rotational–vibrational transitions in the near-infrared; however, these predictions have not been confirmed, despite deep searches[14,15]. Observations[16] with the Infrared Space Observatory (ISO)'s Long Wavelength Spectrometer of the pure rotational $J = 1$–0 ground-state transition at 149.137 μm (where J is total angular momentum) were impaired by the limited resolving power of the spectrometer ($\Delta\lambda = 0.6$ μm), which did not allow the HeH^+ transition to be separated from the nearby Λ-doublet of the methylidyne radical (CH) at 149.09 μm and 149.39 μm.

Very debatable tentative detections of HeH^+ have been reported in the envelope of the supernova SN 1987A[17] and in a high-redshift quasar[18], but all are unconfirmed and are suggested to be considered as upper limits. This lack of direct evidence of the very existence of the molecule has called into question our understanding of the underlying reaction networks[19,20] in local plasmas, and might ultimately invalidate present models of the early Universe.

The deployment of the German Receiver for Astronomy at Terahertz Frequencies (GREAT)[9] heterodyne spectrometer on board the Stratospheric Observatory for Infrared Astronomy (SOFIA)[10] has now opened up new opportunities. Although the HeH^+ $J = 1$–0 transition at 149.137 μm (2010.183873 GHz; ref. [21]) cannot be observed from ground-based observatories, skies become transparent during high-altitude flights with SOFIA. The latest advances in terahertz technologies have enabled the operation of the high-resolution spectrometer upGREAT[22] at frequencies above 2 THz, allowing the HeH^+ $J = 1$–0 line to be targeted. The resolving power of this heterodyne instrument, $\lambda/\Delta\lambda \approx 10^7$, permits the HeH^+ $J = 1$–0 line to be distinguished unambiguously from other, nearby spectral features such as the CH Λ-doublet mentioned previously.

During three flights in May 2016, the telescope was pointed towards NGC 7027 (the total on-target integration time was 71 min). Weak emission in the HeH^+ $J = 1$–0 line was clearly detected (Fig. 1), as was emission from the nearby CH doublet. Notably, the lines are well separated in frequency (Extended Data Fig. 1). The velocity profile of the HeH^+ line matches nicely that of the excited CO $J = 11$–10 transition, which was observed in parallel. The velocity-integrated line brightness temperature, $\int T_{\rm mb}\,{\rm d}v = 3.6 \pm 0.7$ K km s^{-1}, corresponds to a line flux of 1.63×10^{-13} erg s^{-1} cm^{-2}. Because the 14.3″ half-power beam response of upGREAT includes most of the NGC 7027 ionized gas sphere, this result will be close to the total HeH^+ flux emitted in the $J = 1$–0 line. The flux is somewhat higher than the upper limit (1.26×10^{-13} erg s^{-1} cm^{-2}) assigned to any residual HeH^+ contribution in the ISO observations, in the attempt[16] to separate the line from its blend with the CH doublet (see Extended Data Table 1 for the fluxes observed with upGREAT during this experiment).

We have modelled the HeH^+ abundance across NGC 7027. We approximated the nebula as a constant-pressure, spherically symmetric shell, and adjusted the pressure to obtain a Strömgren sphere of angular radius 4.6″—the geometric mean deduced from the 1.4 GHz radio continuum image[23]. We adopted a stellar luminosity of $1.0 \times 10^4\ L_\odot$, a stellar effective temperature of 1.9×10^5 K (ref. [12]), a source distance of 980 parsecs[11], and a He abundance of 0.12 relative to H. Using the CLOUDY photoionization code[24], we calculated profiles of temperature and density (for H, He^+ and electrons) as a function of position across the shell (Fig. 2). The mean electron density within the ionized shell is 4.9×10^4 cm^{-3}, and that in the H/He^+ overlap layer is roughly 2×10^4 cm^{-3}.

We then computed the equilibrium abundance of HeH^+, including the three reactions identified as being important in the layers in which HeH^+ is most abundant[7,13]:

$$He^+ + H \rightarrow HeH^+ + h\nu \quad (1)$$

$$HeH^+ + e^- \rightarrow He + H \quad (2)$$

$$HeH^+ + H \rightarrow H_2^+ + He \quad (3)$$

[1]Max-Planck Institut für Radioastronomie, Bonn, Germany. [2]The Johns Hopkins University, Baltimore, MD, USA. [3]I. Physikalisches Institut, Universität zu Köln, Cologne, Germany. [4]University of Applied Sciences Bonn-Rhein-Sieg, Sankt Augustin, Germany. [5]Institut de Radioastronomie Millimétrique, Saint-Martin-d'Hères, France. *e-mail: rguesten@mpifr-bonn.mpg.de

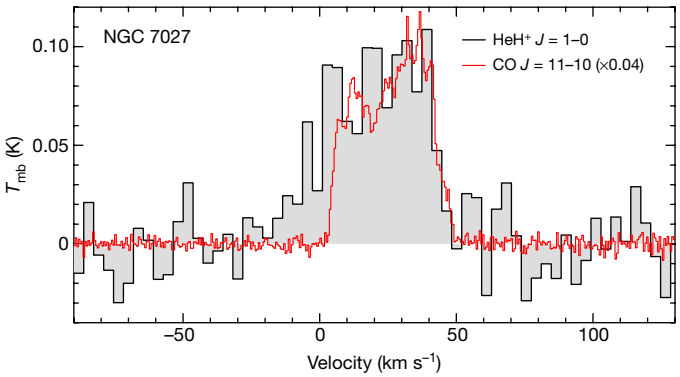

Fig. 1 | Spectrum of the HeH^+ $J = 1-0$ ground-state rotational transition, observed with upGREAT onboard SOFIA pointed towards NGC 7027. 'Contaminating' emission from the nearby but well separated CH Λ-doublet has been removed from the data (see Methods for details of data processing). The spectrum has been rebinned to a resolution of 3.6 km s^{-1} (24 MHz). For comparison, the CO $J = 11–10$ line is superimposed (at a spectral resolution of 0.58 km s^{-1}); this transition was observed in parallel and probes the dense inner edge of the molecular envelope near the ionization front from which the HeH^+ emission is expected to originate. T_{mb}, main-beam brightness temperature. The grey shading shows the area above and below the zero line for each spectral channel.

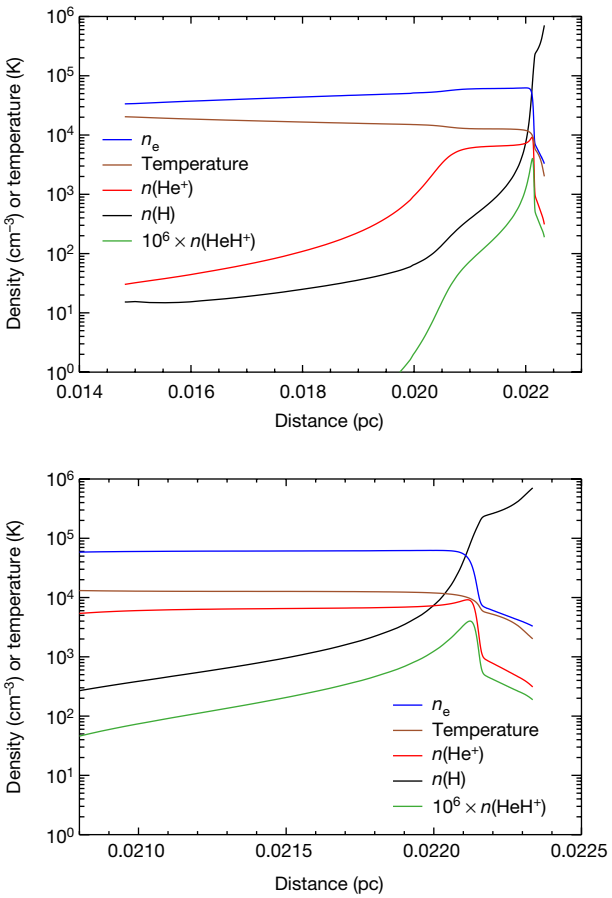

Fig. 2 | Temperature and density profiles for NGC 7027, as predicted by our astrochemical model for this source. The bottom panel presents an expanded view of the top panel. The model assumes a dissociative recombination rate (reaction (2)) of $k_2 = 3.0 \times 10^{-10}\,(T/10^4\,\mathrm{K})^{-0.47}$ cm^3 s^{-1} (see Extended Data Table 2), and a radiative association rate (reaction (1)) of $k_1 = 6.0 \times 10^{-16}$ cm^3 s^{-1}, adjusted to fit the observed $J = 1–0$ line intensity. T, temperature; n, density.

We confirm the conclusion reached previously[13] that, in the planetary nebula environment, the reaction $He + H^+ \rightarrow HeH^+ + h\nu$—which dominates HeH^+ formation in the early Universe—can be neglected, as can the reaction $H_2^+ + He \rightarrow HeH^+ + H$ ($h\nu$ is the photon energy). Moreover, we confirm that the photodissociation of HeH^+ is slow compared with reactions (2) and (3) in the region in which the HeH^+ emission arises, and can therefore also be neglected. For the reactions (1), (2) and (3), we critically reviewed the most recent available estimates for the rate coefficients, as detailed in Extended Data Table 2. Published values for the rate coefficient k_1 for the radiative association reaction (reaction (1)) vary widely; here we adopt a value of 1.4×10^{-16} cm^3 s^{-1}, based on the most recently published cross-section[25]. Experimental studies[26,27] of the dissociative recombination reaction (reaction (2))—involving measurements of the cross-section at energies up to 40 electronvolts (eV)—derive values for the thermal rate coefficient (k_2) that are plainly inconsistent with the cross-sections presented in that same study. A reanalysis[26] of those measurements yields $k_2 = 3.0 \times 10^{-10}$ cm^3 s^{-1} (at a kinetic temperature of 10^4 K)—a value that is much smaller than that originally inferred from the measurements. To compute the emissivity of the HeH^+ $J = 1–0$ transition, we made use of recent estimates for the rate coefficients for electron-impact excitation[28]. At the densities of relevance to NGC 7027, collisional de-excitation can be neglected, and the $J = 1–0$ emissivity is determined by the total rate of excitation from $J = 0$ to all states with $J > 0$, for which we obtain a value of 2.8×10^{-7} $(T/10^4\,\mathrm{K})^{-0.5}$ cm^3 s^{-1} (where T is the temperature).

Given the rate coefficients discussed above, our model predicts an integrated main-beam brightness temperature of 0.86 K km s^{-1}, a factor of roughly four below the value we observe. The most uncertain of the rate coefficients is probably k_1; if we take the approach of adjusting its value to fit the observed line intensity, we obtain $k_1 = 6.0 \times 10^{-16}$ cm^3 s^{-1}. Figure 2 shows the results obtained using this value. As expected, the production of HeH^+ peaks sharply in the He^+/H overlap layer, reaching a peak abundance relative to H nuclei of 4.0×10^{-8}. The column density from the centre to the edge of the nebula is 2.4×10^{12} cm^{-2}; the total line flux emitted by NGC 7027 in the $J = 1 - 0$ transition, based on the model, is 2.1×10^{-13} erg s^{-1} cm^{-2}. For the infrared rovibrational lines, we compute fluxes that are consistent with previous nondetections. For the $v = 1–0$ R(0) line, observed using a circular aperture of 8″ that did not fully encompass the source[14], the predicted flux of 1.3×10^{-14} erg s^{-1} cm^{-2} is roughly three times less than the observed upper limit. For the $v = 1–0$ P(2) line, the flux predicted in a $0.87 \times 10.3''$ slit is 5.9×10^{-15} erg s^{-1} cm^{-2}, comparable to the reported[15] upper limit of 5×10^{-15} erg s^{-1} cm^{-2}.

Comparing the observed $J = 1–0$ flux with the predictions of our excitation model in the well constrained physical environment of the NGC 7027 nebula casts light on the relative importance of the different mechanisms for the formation and destruction of the helium hydride ion, and in particular constrains the radiative association rate (reaction (1)) and the dissociative recombination rate (reaction (2)). In view of the large discrepancies reported in the literature, and because our model based on the latest cross-sections underpredicts the observed line fluxes, our findings may stimulate further studies of these reactions (and of the corresponding radiative association of He and H^+ that dominates under the conditions of the early Universe). The validation of these uncertain values by our astronomical measurements is limited by the relative simplicity of our physical model for the source; as in previous modelling efforts[12], we have approximated an elongated nebula as being spherically symmetrical. Future non-spherically symmetrical models could refine our estimates, but are beyond the scope of this study.

Although HeH^+ is of limited importance on Earth today, the chemistry of the Universe began with this ion. The lack of definitive evidence for its very existence in interstellar space has been a dilemma for astronomy. The unambiguous detection reported here brings a decades-long search to a happy ending at last—a success that has become possible thanks to maturing terahertz technologies (incorporated in the upGREAT instrument) and the timely availability of the unique SOFIA

observatory, which allows high-altitude flights above the absorbing layers of Earth's atmosphere.

Online content

Any methods, additional references, Nature Research reporting summaries, source data, statements of data availability and associated accession codes are available at https://doi.org/10.1038/s41586-019-1090-x.

Received: 6 January 2019; Accepted: 11 February 2019;
Published online 17 April 2019.

1. Galli, D. & Palla, F. The dawn of chemistry. *Annu. Rev. Astron. Astrophys.* **51**, 163–206 (2013).
2. Lepp, S., Stancil, P. C. & Dalgarno, A. Atomic and molecular processes in the early Universe. *J. Phys. B* **35**, R57–R80 (2002).
3. Hogness, T. R. & Lunn, E. G. The ionization of hydrogen by electron impact as interpreted by positive ray analysis. *Phys. Rev.* **26**, 44–55 (1925).
4. Drabowski, I. & Herzberg, G. The predicted infrared spectrum of HeH^+ and its possible astrophysical importance. *Ann. NY Acad. Sci.* **38**, 14–25 (1977).
5. Black, J. H. Molecules in planetary nebulae. *Astrophys. J.* **222**, 125–131 (1978).
6. Flower, D. R. & Roueff, E. On the formation and destruction of HeH^+ in gaseous nebulae and the associated infra-red emission line spectrum. *Astron. Astrophys.* **72**, 361–366 (1979).
7. Roberge, W. & Dalgarno, A. The formation and destruction of HeH^+ in astrophysical plasmas. *Astrophys. J.* **255**, 489–496 (1982).
8. Heyminck, S. et al. GREAT: the SOFIA high-frequency heterodyne instrument. *Astron. Astrophys.* **542**, L1 (2012).
9. Risacher, C. et al. First supra-THz heterodyne array receivers for astronomy with the SOFIA observatory. *IEEE Trans. Terahertz Sci. Technol.* **6**, 199–211 (2016).
10. Young, E. T. et al. Early science with SOFIA, the Stratospheric Observatory for Infrared. *Astrophys. J.* **749**, L17 (2012).
11. Masson, C. R. The structure of NGC 7027 and a determination of its distance by measurement of proper motions. *Astrophys. J.* **336**, 294–303 (1989).
12. Zijlstra, A. A., van Hoof, P. A. M. & Perley, R. A. The evolution of NGC 7027 at radio frequencies: a new determination of the distance and core mass. *Astrophys. J.* **681**, 1296–1309 (2008).
13. Cecchi-Pestellini, C. & Dalgarno, A. Emission of HeH^+ in nebulae. *Astrophys. J.* **413**, 611–618 (1993).
14. Moorhead, J. M., Lowe, R. P., Maillard, J.-P., Wehlau, W. H. & Bernath, P. F. Search for HeH^+ in NGC 7027. *Astrophys. J.* **326**, 899–904 (1988).
15. Dinerstein, H. L. & Geballe, T. R. Detection and significance of [Zn IV] 3.625 microns in planetary nebulae. *Astrophys. J.* **562**, 515–520 (2001).
16. Liu, X.-W. et al. An ISO long wavelength spectrometer detection of CH in NGC 7027 and a HeH^+ upper limit. *Mon. Not. R. Astron. Soc.* **290**, L71–L75 (1997).
17. Miller, S., Tennyson, J., Lepp, S. & Dalgarno, A. Identification of features due to H_3^+ in the infrared spectrum of supernova 1987A. *Nature* **355**, 420–422 (1992).
18. Zinchenko, I., Dubrovich, V. & Henkel, C. A search for HeH^+ and CH in a high-redshift quasi-stellar object. *Mon. Not. R. Astron. Soc.* **415**, L78–L80 (2011).
19. Loreau, J., Vranckx, S., Desouter-Lecomte, M., Vaeck, N. & Dalgarno, A. Photodissociation and radiative association of HeH^+ in the metastable triplet state. *J. Phys. Chem. A* **117**, 9486–9492 (2013).
20. Zicler, E. et al. Search for hydrogen-helium molecular species in space. *Astron. Astrophys.* **607**, A61 (2017).
21. Perry, A. J., Hodges, J. N., Markus, C. R., Kocheril, G. S. & McCall, B. J. High precision sub-Doppler infrared spectroscopy of the HeH^+ ion. *J. Chem. Phys.* **141**, 101101 (2014).
22. Risacher, C. et al. The upGREAT 1.9 THz multi-pixel high resolution spectrometer for the SOFIA Observatory. *Astron. Astrophys.* **595**, A34 (2016).
23. Basart, J. P. & Daub, C. T. Temperature and emission-measure distributions for several planetary nebulae. *Astrophys. J.* **317**, 412–422 (1987).
24. Ferland, G. J. et al. The 2013 Release of Cloudy. *Rev. Mex. Astron. Astrofis.* **49**, 137–163 (2013).
25. Vranckx, S., Loreau, J., Desouter-Lecomte, M. & Vaeck, N. Determination of photodissociation and radiative association cross sections from the same time-dependent calculation. *J. Phys. B* **46**, 155201 (2013).
26. Novotný, O. et al. Dissociative recombination measurements of HCl^+ using an ion storage ring. *Astrophys. J.* **777**, 54–68 (2013).
27. Strömholm, C. et al. Dissociative recombination and dissociative excitation of $4HeH^+$: absolute cross sections and mechanisms. *Phys. Rev. A* **54**, 3086–3094 (1996).
28. Čurík, R. & Greene, C. H. Inelastic low-energy collisions of electrons with HeH^+. *J. Chem. Phys.* **147**, 054307 (2017).

Acknowledgements upGREAT is a development by the Max-Planck Institut (MPI) für Radioastronomie and the Kölner Observatorium für SubMillimeter Astronomie (KOSMA)/Universität zu Köln, in cooperation with the Deutsches Zentrum für Luft- und Raumfahrt (DLR; German Aerospace Center) Institut für Optische Sensorsysteme. The development of upGREAT is financed by the participating institutes, by the German Aerospace Center (DLR) under grants 50 OK 1102, 1103 and 1104, and within the Collaborative Research Centre 956, funded by the Deutsche Forschungsgemeinschaft (DFG). The work of D.N. was supported by grant 120364 from NASA's Astrophysical Data Analysis Program (ADAP). SOFIA is jointly operated by the Universities Space Research Association (USRA), under NASA contract NAS2-97001, and the Deutsches SOFIA Institut (DSI), under DLR contracts 50 OK 0901 and 50 OK 1301 to the University of Stuttgart. We thank the SOFIA operations and engineering teams for their dedication and supportive responses to our requests, and E. Young and G. Sandell for making these observations possible. We are grateful to O. Novotny for recomputing the thermal rate coefficient for the dissociative recombination of HeH^+, using published experimental merged-beam cross-section measurements in the literature[27]. We thank J. Loreau for providing published cross-section calculations for the radiative association reaction (reaction (1)) in tabular form, and for clarifying that these cross-sections apply specifically to collisions of H (1*s*) and He^+ (1*s*) in the singlet state.

Reviewer information *Nature* thanks Michael Barlow and Stephen Lepp for their contribution to the peer review of this work.

Author contributions R.G. initiated and planned the observations. H.W. calibrated the data. D.N. performed astrochemical modelling. R.G., H.W., K.M.M. and D.N. wrote the text. Extending the reception bandwidth of the upGREAT receiver to frequencies beyond 2 THz has been a joint year-long effort by the GREAT team. All authors contributed to the interpretation of the data and commented on the final manuscript.

Competing interests The authors declare no competing interests.

Additional information
Extended data is available for this paper at https://doi.org/10.1038/s41586-019-1090-x.
Reprints and permissions information is available at http://www.nature.com/reprints.
Correspondence and requests for materials should be addressed to R.G.
Publisher's note: Springer Nature remains neutral with regard to jurisdictional claims in published maps and institutional affiliations.

METHODS

SOFIA/GREAT observations. The planetary nebula NGC 7027 (right ascension 21 h 07 min 01.59 s; declination 42° 14′ 10.2″; J2000) was observed with the GREAT[8] heterodyne spectrometer during three flights between 14 and 25 May 2016 out of Palmdale, USA. The seven-pixel array receiver upGREAT/LFA-H[9], tuned to the frequency of the HeH^+ $J = 1–0$ transition at 149.13 μm (2010.1839 GHz), was operated in parallel with the L1 channel, which was recording the CO $J = 11–10$ transition for reference. Tuning the *H*-polarization of the array to the HeH^+ frequency has become possible with the installation of a new solid-state local oscillator reference source (developed by Virginia Diodes Inc.), just before this flight series. The NbN-based hot electron bolometer mixers[29] of upGREAT operate at unmatched low-noise temperatures of 850 K double sideband (DSB), with a 3-dB noise bandwidth of the intermediate frequency of 3.7 GHz. The signals were processed with our digital 4-GHz wideband monolithic fast Fourier transform (FFT) spectrometers[30], operating 16*k* channels (with 244 kHz spectral resolution) for each of the front-end channels. Unless noted, all spectra presented here have been box-smoothed to a spectral resolution of 24.4 MHz, as appropriate for the velocity width of the source.

The instrument was operated in double-beam chopped mode, with a beam throw of 40″, at a chop rate of 2.5 Hz. Pointing was established by the telescope operators on nearby optical reference stars, to an accuracy of 1″–2″. Before the flight series, the optical axis of the GREAT instrument had been aligned to these imagers by observations of Jupiter. The main beam-coupling efficiencies for the L1 channel and the upGREAT/LFA-H receiver, also determined towards Jupiter, are 0.66 for both. The half-power beam widths (HPBWs) of GREAT at 2010.18 GHz and 1267.01 GHz are 14.3″ and 21.1″, respectively, and are diffraction limited for the 2.5-m SOFIA telescope.

The observations were performed at flight altitudes of between 40 thousand and 43 thousand feet; atmospheric conditions were typical for late-spring flights out of Palmdale, with a residual water-vapour column of roughly 20 μm. This resulted in typical single-sideband system temperatures, T_{sys}, of 1,800 K.

Observing strategy. As the upGREAT heterodyne spectrometer is sensitive to signals from both sidebands of the mixer, it detects a response from both mixing products, $\nu_{LO} \pm \nu_{IF}$, where ν_{LO} is the frequency of the local oscillator reference signal, and ν_{IF} is the intermediate frequency (usable range 0.3–4 GHz). The HeH^+ observations were performed in the 'upper sideband' (USB; $\nu_{LO} < \nu_{HeH^+}$), because tuning the line into the lower sideband would pick up excess noise from strong atmospheric emission in the image band. To exclude any chance coincidence with contamination from the image sideband, and thereby a faulty assignment of transitions, it is common practice in detection experiments to verify the assignments with observations of shifted intermediate-frequency reference signals. The first part of our observation was performed with an intermediate-frequency offset of 1.4 GHz; confirmatory observations made during the second and third flights used an offset of 1.2 GHz (this shifted any feature from the image band by -60 km s^{-1}).

Calibration and analysis. Calibration of the HeH^+ data was challenging. The line is affected by the proximity of a rather narrow ozone line at 2,009.9 GHz that is optically thick at the line's centre. Because the line originates in the signal band, the only way to minimize its impact is to use the seasonal variation of the Doppler correction. In May, the line had moved out of the expected velocity range of NGC 7027; in the autumn, however, it would be blending its core velocities, making this detection experiment impossible.

We corrected the spectrum for atmospheric losses following the usual calibration scheme[31], using two load signals (at ambient temperature and a cold temperature to determine the instrument gain) plus a blank sky signal, which allows us to fit an atmospheric model to the observed sky emission. The transmission thus obtained is then used to correct the observed astronomical signal to the level it has outside the atmosphere. Although the applied method proves adequate to correct for the broad absorption features that result from water vapour and collision-induced absorption by N_2 and O_2, it fails to provide a close fit to the prominent ozone line. We therefore deduced the absorption profile of this line directly from its observed emission, assuming that it originates mainly from a stratospheric layer with a constant source function.

Data analysis. As mentioned previously, the high spectral resolution of upGREAT is essential to separate the HeH^+ $J = 1–0$ line from nearby transitions of the methylidyne radical, CH. HeH^+ is offset by only -619 MHz ($+92$ km s^{-1}) from the group of hyperfine transitions of the upper CH $^2\Pi_{½}$ $J = 3/2–1/2$ Λ-doublet. With a Λ-splitting of roughly 4.05 GHz, the lower Λ-doublet will unavoidably blend from the image band into our spectrum. The frequency set-up for our observations was optimized before the actual flights, by simulating the blends of molecular transitions superposed on the atmospheric transmission. In Extended Data Fig. 1 we display the calibrated 'raw' spectra, as observed in the two frequency settings. The positions of the CH hyperfine transitions and of the HeH^+ $J = 1–0$ line are marked, corrected for the systemic source velocity of NGC 7027 ($V_{lsr} = 26$ km s^{-1}). The sky transmission is superimposed, displaying also the strong telluric (ozone) absorption at positive velocities.

Data availability

The data presented here are available through the SOFIA data archive at https://dcs.arc.nasa.gov/ and can be retrieved by searching for the project identification code, 83_0405.

29. Pütz, P., Büchel, D., Jacobs, K., Schultz, M. & Honingh, C. 1.9 THz waveguide HEB mixers for the upGREAT low frequency array. In *Proc. 26th Int. Symp. Space THz Technology* (eds Blundell, R. & Mehdi, I.) (Cambridge, MA, USA, 2015)
30. Klein, B. et al. High-resolution wide-band fast Fourier transform spectrometers. *Astron. Astrophys.* **542**, L3 (2012).
31. Guan, X. et al. GREAT/SOFIA atmospheric calibration. *Astron. Astrophys.* **542**, L4 (2012).
32. Müller, H. S. P., Schlöder, F., Stutzki, J. & Winnewisser, G. The Cologne Database for Molecular Spectroscopy, CDMS: a useful tool for astronomers and spectroscopists. *J. Mol. Struct.* **742**, 215–227 (2005).
33. Davidson, S. A., Evenson, K. M. & Brown, J. M. A measurement of the rotational spectrum of the CH radical in the far-infrared. *Astrophys. J.* **546**, 330–337 (2001).
34. Matsushima, F., Oka, T. & Takagi, K. Observation of the rotational spectra of $4HeH^+$, $4HeD^+$, $3HeH^+$, and $3HeD^+$. *Phys. Rev. Lett.* **78**, 1664–1666 (1997).
35. Bovino, S., Tacconi, M., Gianturco, F. A. & Galli, D. Ion chemistry in the early universe. Revisiting the role of HeH^+ with new quantum calculations. *Astron. Astrophys.* **529**, A140 (2011).
36. Stancil, P. C., Lepp, S. & Dalgarno, A. The deuterium chemistry of the early Universe. *Astrophys. J.* **509**, 1–10 (1998).
37. Zygelman, B. & Dalgarno, A. The radiative association of He^+ and H. *Astrophys. J.* **365**, 239–240 (1990).

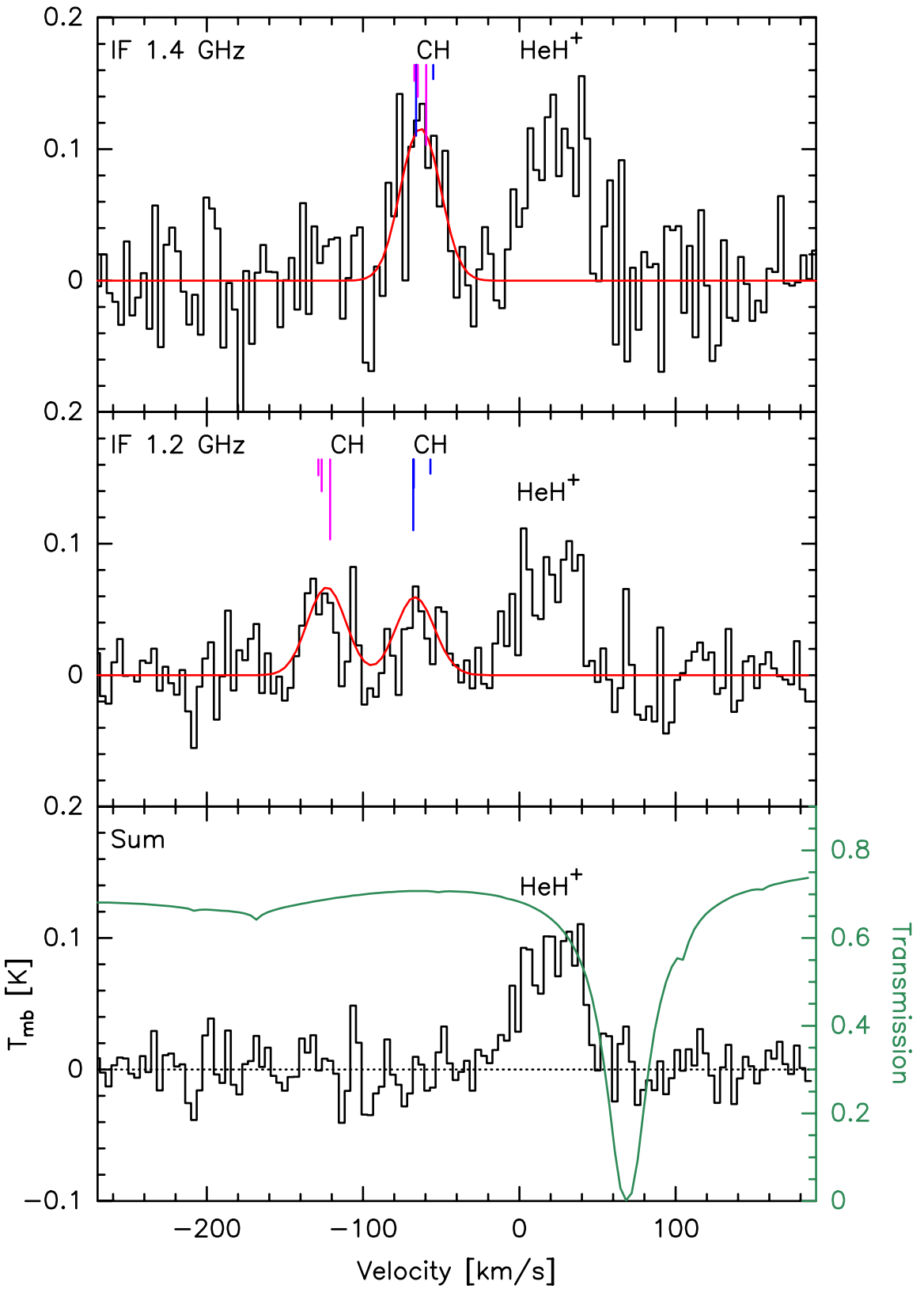

Extended Data Fig. 1 | Calibrated and baseline-corrected, but otherwise unprocessed, spectra observed in two different intermediate-frequency set-ups (ν_{IF} = 1.4 GHz and 1.2 GHz). See text for details. The frequencies of the group of hyperfine transitions of the CH Λ-doublets are marked (blue, upper doublet from the signal band; purple, lower-doublet blending from the image band). A pattern fit (optically thin, with intensities of the hyperfine pattern as per Extended Data Table 1) is superposed with red lines. The bottom spectrum displays the co-added residuals of the two observations, after removal of the CH emission (shown is the residual after removal of the Gaussian fits). The atmospheric transmission is shown with a green line, for typical conditions encountered in May 2016 (precipitable water-vapour column 20 μm; opacity of dry atmospheric constituents scaled by a factor of 1.4 with respect to the reference model, for a sightline at 35° elevation).

Extended Data Table 1 | Molecular line parameters and line intensities as observed here

Transition $^2\Pi_J$	hfs F^p	ν_{hfs} [GHz]	λ_{hfs} [μm]	relative line strength	line intensity [K km/s]
CH $^2\Pi_{3/2} \rightarrow {}^2\Pi_{1/2}$	$1^- \rightarrow 1^+$	2006.7488646	149.392	0.2	1.5 (0.3)
	$1^- \rightarrow 0^+$	2006.7625778	149.391	0.4	
	$2^- \rightarrow 1^+$	2006.7990641	149.308	1.0	
	$1^+ \rightarrow 1^-$	2010.7385887	149.096	0.2	1.5 (0.3)
	$1^+ \rightarrow 0^-$	2010.8104600	149.090	0.4	
	$2^+ \rightarrow 1^-$	2010.8119200	149.090	1.0	
HeH^+ (J=1-0)		2010.1838730	149.137	--	3.6 (0.7)

The molecular line parameters have been taken from the Cologne Database for Molecular Spectroscopy[32], where the origin of the CH (ref. [33]) and HeH^+ (ref. [34]) frequencies is discussed. Velocity-integrated line intensities were derived using the CLASS software package (http://www.iram.fr/IRAMFR/GILDAS). To the HeH^+ line we assign an absolute flux uncertainty of 20%, which is dominated by the challenging calibration at the edge of the strong though narrow telluric absorption (see Extended Data Fig. 1). The CH doublets are fit using the relative strengths between the hyperfine transitions. For the decomposition of the two intermediate-frequency settings, we assume equal intensity for the two groups of hyperfine transitions; the different calibration in the two sidebands has been taken into account. hfs, hyperfine structure transition; *F* is the total angular momentum quantum number and *p* its parity.

Extended Data Table 2 | Reaction rates used herein

Reaction	Rate coefficient [$cm^3\ s^{-1}$]	Notes
$He^+ + H \rightarrow HeH^+ + h\nu$	1.4×10^{-16}	1
$HeH^+ + e \rightarrow He + H$	$3.0 \times 10^{-10}\ (T/10^4\ K)^{-0.47}$	2
$HeH^+ + H \rightarrow He + H_2^+$	$1.2 \times 10^{-9}\ (T/10^4\ K)^{-0.11}$	3

(1) The rate coefficient (in $cm^3\ s^{-1}$) was obtained by averaging the published cross-sections[25] over a Maxwell–Boltzmann distribution, and applies to temperatures in the range 5,000 K to 20,000 K. The published cross-sections are for collisions in which He^+ (1*s*) and H (1*s*) are in the singlet state (total spin 0), but as only one-quarter of collisions will have spin 0, the rate has been reduced by a factor of four. Values in the literature[13,36,37] vary widely. (2) This value corrects an error in the computation[27] of the thermal rate coefficient from the cross-section measurements. Taking as valid the primary data of ref. [27], namely, the merged-beam cross-sections given in their figure 3, the thermal rate coefficients was recomputed by applying the methods developed;, for example, for the calculation of the dissociative recombination cross-section of HCl^+ (ref. [26]); we find the thermal rate coefficient to be an order of magnitude below that originally computed[27]. (3) Ref. [35] shows the rate coefficient obtained from quantum calculations.